Available online at www.sciencedirect.com

ScienceDirect

Chinese Journal of Aeronautics 23(2010) 235-239

Chinese Journal of Aeronautics

www.elsevier.com/locate/cja

Polynomial Representation of NURBS and Its Application to High Frequency Scattering Prediction

Fang Xiang, Su Donglin

School of Electronics and Information Engineering, Beijing University of Aeronautics and Astronautics, Beijing 100191, China

Received 26 March 2009; accepted 7 July 2009

Abstract

This article presents a method that uses physical optics (PO) techniques to compute the monostatic radar cross section (RCS) of electrically large conducting objects modeled by non-uniform rational B-spline (NURBS) surfaces. At the beginning, a new algorithm to convert recursive B-spline basis function into piecewise polynomials in power form is presented. Then, algorithm computes the polynomial representation of B-spline basis functions and NURBS surface geometric parameters are obtained. The PO integral over NURBS surfaces of an electrically large conducting object is used to predict the object's RCS. The NURBS surface is divided into small piecewise polynomial parametric patches by isoparametric curves, and the PO integral expression over the parametric domain of each polynomial parametric patch is reduced to an analytical expression which permits an accurate and effective computation of the PO integral by using a modified Ludwig's algorithm. The RCS of the object can be obtained by adding up the PO integral contribution of each polynomial parametric patch. The effectiveness of this method is verified by numerical examples.

Keywords: splines; polynomial representation; electromagnetic wave scattering; radar cross section; physical optics; Ludwig's algorithm

1. Introduction

The non-uniform rational B-spline (NURBS) surface modeling technique is currently widely used in aeronautic, automobile, ship and other industries because it provides great advantages in geometrical representation for complex objects. A NURBS-based description is of particular use when treating problems of electromagnetic scattering from large conducting surfaces in the framework of high-frequency techniques like physical optics (PO)[1] and the uniform theory of diffraction (UTD)[2-3]. The PO technique requires the computation of double integrals with fast oscillating kernels, and the use of NURBS for describing complex surfaces can alleviate the numerical problems by constructing efficient quasi-analytical tools such as the stationary phase integration method[1,4], curvilinear integral approximation[5], ribbon integration technique[6], splitting extrapolation method[7], current modes approach[8-9] and Ludwig's algorithm[10-11]. When dealing with large and complex bodies, a combination of geometrical optics (GO) and PO[12] or a new PO approach based on electric and magnetic currents[13] can be used for the multiple reflections analysis.

The numerical computation of geometrical parameters, such as point coordinates and parametric derivatives, would be easily performed if each NURBS surface is transformed into a set of rational Bezier patches via the Cox-De Boor algorithm[14]. This is due to the Bernstein polynomials characteristic of more numerical stability with respect to the B-spline bases[1]. For this reason, high-frequency techniques such as PO are not usually applied to a NURBS surface directly but rather to the rational Bezier patches making up the NURBS surface[1-4,10-13].

This article applies the PO integral to the monostatic radar cross section (RCS) computation of electrically large perfect conducting objects modeled with NURBS surfaces. B-spline basis functions are expressed through piecewise polynomials. The obtained expressions of the coefficients of the polynomials are constant on the various knot spans. The straightforward polynomial representation of B-spline bases makes it easy to evaluate the PO integral directly over a NURBS surface by means of an efficient quasi-analytical tool. A modified Ludwig's algorithm is adopted

*Corresponding author. Tel.: +86-10-82317223.
E-mail address: xiangfangit@ee.buaa.edu.cn
Foundation items: National Natural Science Foundation of China (60831001); Innovation Foundation of Beijing University of Aeronautics and Astronautics for PhD Graduates

doi: 10.1016/S1000-9361(09)60210-7

to evaluate the PO integral. Numerical results show the effectiveness of this method.

2. Polynomial Representation of NURBS

2.1. Definition and polynomial representation of B-spline basis functions

Let $\boldsymbol{U}=[u_0 \quad u_1 \quad \cdots \quad u_m]$ be a vector which consists of a non-decreasing sequence of real numbers, i.e. $u_i \le u_{i+1}$ (i=0,1,⋯, m−1), u_i is knot and $\boldsymbol{U}$ the knot vector. The ith B-spline basis function of p-degree (order p+1), denoted by $N_{i,p}(u)$, is defined as[15]

$$\left.\begin{aligned} N_{i,0}(u) &= \begin{cases} 1 & u_i \le u \le u_{i+1} \\ 0 & \text{otherwise} \end{cases} \\ N_{i,p}(u) &= \frac{u-u_i}{u_{i+p}-u_i} N_{i,p-1}(u) + \\ &\quad \frac{u_{i+p+1}-u}{u_{i+p+1}-u_{i+1}} N_{i+1,p-1}(u) \end{aligned}\right\} \tag{1}$$

In this article, $N_{i,p}(u)$ can also be expressed through the following polynomial:

$$N_{i,p}(u) = \sum_{k=0}^{p} C_{i,p,k}(u) u^k \tag{2}$$

The expression of the coefficients of the polynomial $C_{i,p,k}$ can be obtained by combining Eq.(1) and Eq.(2):

$$\left.\begin{aligned} C_{i,0,0}(u) &= N_{i,0}(u) \\ C_{i,p,0}(u) &= \frac{u_{i+p+1}}{u_{i+p+1}-u_{i+1}} C_{i+1,p-1,0}(u) - \\ &\quad \frac{u_i}{u_{i+p}-u_i} C_{i,p-1,0}(u) \\ C_{i,p,p}(u) &= \frac{1}{u_{i+p}-u_i} C_{i,p-1,p-1}(u) - \\ &\quad \frac{1}{u_{i+p+1}-u_{i+1}} C_{i+1,p-1,p-1}(u) \\ C_{i,p,k}(u) &= \frac{C_{i,p-1,k-1}(u)-u_i C_{i,p-1,k}(u)}{u_{i+p}-u_i} - \\ &\quad \frac{C_{i+1,p-1,k-1}(u)-u_{i+p+1} C_{i+1,p-1,k}(u)}{u_{i+p+1}-u_{i+1}} \\ &\quad (1 \le k \le p-1) \end{aligned}\right\} \tag{3}$$

Note that those coefficients depend only on the knot span $[u_i, u_{i+1})$ where u lies, i.e., they have a constant value on the various knot spans，as shown in Fig.1. Consequently, the derivative of $N_{i,p}$ is obtained as follows:

$$\frac{\mathrm{d}N_{i,p}(u)}{\mathrm{d}u} = N_{i,p}^{u}(u) = \sum_{k=1}^{p} k C_{i,p,k}(u) u^{k-1} \tag{4}$$

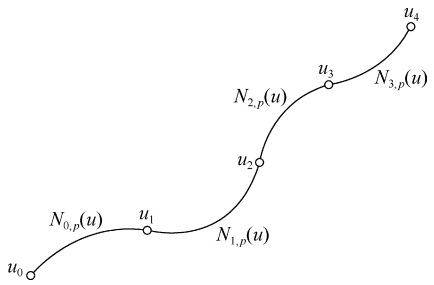

Fig.1 Piecewise polynomial representation of NURBS.

2.2. Definition of NURBS surfaces

A NURBS surface of p-degree in the u direction and of q-degree in the v direction is a bivariate vector-valued piecewise rational function in the following form[15]:

$$\boldsymbol{r}(u,v) = \frac{\sum_{i=0}^{n}\sum_{j=0}^{m} N_{i,p}(u) N_{j,q}(v) w_{i,j} \boldsymbol{P}_{i,j}}{\sum_{i=0}^{n}\sum_{j=0}^{m} N_{i,p}(u) N_{j,q}(v) w_{i,j}} \quad (0 \le u,v \le 1) \tag{5}$$

where $\boldsymbol{P}_{i,j}$ is a bidirectional control net, $w_{i,j}$ the weight, $N_{i,p}(u)$ and $N_{j,q}(v)$ are the NURBS basis functions defined on the knot vectors

$$\boldsymbol{U} = \left[\underbrace{0 \ \cdots \ 0}_{p+1} \quad u_{p+1} \quad \cdots \quad u_{r-p-1} \quad \underbrace{1 \ \cdots \ 1}_{p+1}\right]$$

$$\boldsymbol{V} = \left[\underbrace{0 \ \cdots \ 0}_{q+1} \quad v_{q+1} \quad \cdots \quad v_{s-q-1} \quad \underbrace{1 \ \cdots \ 1}_{q+1}\right]$$

where $r = n+p+1$ and $s = m+q+1$.

The polynomial representation can also be applied to the parametric space of the NURBS surfaces with the following formulas for the first order derivatives $\boldsymbol{r}_u(u,v)$ and $\boldsymbol{r}_v(u,v)$ of a NURBS surface:

$$\boldsymbol{r}_u(u,v) = \frac{\boldsymbol{A}_u(u,v) - w_u(u,v)\boldsymbol{r}(u,v)}{\sum_{i=0}^{n}\sum_{j=0}^{m} N_{i,p}(u) N_{j,q}(v) w_{i,j}} \tag{6}$$

$$\boldsymbol{r}_v(u,v) = \frac{\boldsymbol{A}_v(u,v) - w_v(u,v)\boldsymbol{r}(u,v)}{\sum_{i=0}^{n}\sum_{j=0}^{m} N_{i,p}(u) N_{j,q}(v) w_{i,j}} \tag{7}$$

$$\boldsymbol{A}_u(u,v) = \sum_{i=0}^{n}\sum_{j=0}^{m} N_{i,p}^{u}(u) N_{j,q}(v) w_{i,j} \boldsymbol{P}_{i,j} \tag{8}$$

$$\boldsymbol{A}_v(u,v) = \sum_{i=0}^{n}\sum_{j=0}^{m} N_{i,p}(u) N_{j,q}^{v}(v) w_{i,j} \boldsymbol{P}_{i,j} \tag{9}$$

$$w_u(u,v) = \sum_{i=0}^{n}\sum_{j=0}^{m} N_{i,p}^{u}(u) N_{j,q}(v) w_{i,j} \tag{10}$$

$$w_v(u,v)=\sum_{i=0}^{n}\sum_{j=0}^{m}N_{i,p}(u)N_{j,q}^{v}(v)w_{i,j} \tag{11}$$

$$N_{i,p}^{u}(u)=\sum_{k=1}^{p}kC_{i,p,k}(u)u^{k-1} \tag{12}$$

$$N_{j,q}^{v}(v)=\sum_{k=1}^{q}kC_{j,q,k}(v)v^{k-1} \tag{13}$$

Then, the B-spline basis functions of polynomial form defined by Eq.(2) and Eq.(3) make the computation of surface geometrical parameters, such as point coordinates and parametric derivatives more convenient than those of recurrence form defined by Eq.(1).

3. RCS Computation with PO Method

Under the illumination of a monochromatic plane wave, according to the far field approximation, the RCS of an arbitrary conducting body modeled with NURBS surfaces predicted by PO is given by[10]

$$\sigma=\frac{4\pi}{\lambda^2}|I|^2 \tag{14}$$

$$I=\int_0^1\int_0^1\{\hat{\boldsymbol{k}}_{\mathrm{w}}\cdot[\boldsymbol{r}'_u(u,v)\times\boldsymbol{r}'_v(u,v)\}\cdot \mathrm{e}^{-\mathrm{j}2k_{\mathrm{w}}\hat{\boldsymbol{k}}_{\mathrm{w}}\boldsymbol{r}'(u,v)}]\mathrm{d}u\mathrm{d}v \tag{15}$$

where λ is the wavelength, $\hat{\boldsymbol{k}}_{\mathrm{w}}$ the normalized wave vector, $k_{\mathrm{w}}=2\pi/\lambda$ the free space wave number. The surface points $\boldsymbol{r}'(u,v)$ are determined by Eq.(5), and the parametric derivatives $\boldsymbol{r}'_u(u,v)$, $\boldsymbol{r}'_v(u,v)$ by Eq.(6) and Eq.(7). Eq.(15) can be rewritten into

$$I=\int_0^1\int_0^1 F(u,v)\mathrm{e}^{\mathrm{j}k_{\mathrm{w}}\gamma(u,v)}\mathrm{d}u\mathrm{d}v \tag{16}$$

where $F(u,v)=\hat{\boldsymbol{k}}_{\mathrm{w}}\cdot[\boldsymbol{r}'_u(u,v)\times\boldsymbol{r}'_v(u,v)]$, $\gamma(u,v)=-2\,\hat{\boldsymbol{k}}_{\mathrm{w}}\cdot\boldsymbol{r}'(u,v)$.

The double integral in Eq.(16) over a Bezier patch can be solved with a modified Ludwig's algorithm[10]. For a NURBS surface defined by Eq.(5), the parametric domain [0,1]×[0,1] can be converted into a rectangular grid made of $M\times N$ sub-domains using equispaced isoparametric lines both in the u direction and in the v direction. Thus, the integral in Eq.(16) over a NURBS surface can be divided into integrals over small parametric sub-domains:

$$I=\int_0^1\int_0^1 F(u,v)\mathrm{e}^{\mathrm{j}k_{\mathrm{w}}\gamma(u,v)}\mathrm{d}u\mathrm{d}v= \sum_{m=0}^{M-1}\sum_{n=0}^{N-1}\int_{m/M}^{(m+1)/M}\int_{n/N}^{(n+1)/N}F(u,v)\mathrm{e}^{\mathrm{j}k_{\mathrm{w}}\gamma(u,v)}\mathrm{d}u\mathrm{d}v \tag{17}$$

Let $\Delta E_{mn}=\int_{m/M}^{(m+1)/M}\int_{n/N}^{(n+1)/N}F(u,v)\mathrm{e}^{\mathrm{j}k_{\mathrm{w}}\gamma(u,v)}\mathrm{d}u\mathrm{d}v$. The functions F and γ can be respectively approximated by a simple linear form over the parametric sub-domain $[m/M,(m+1)/M]\times[n/N,(n+1)/N]$.

$$F(u,v)\approx a_{mn}+b_{mn}(u-\frac{m}{M})+c_{mn}(v-\frac{n}{N}) \tag{18}$$

$$\gamma(u,v)\approx \alpha_{mn}+\beta_{mn}(u-\frac{m}{M})+\xi_{mn}(v-\frac{n}{N}) \tag{19}$$

where

$$a_{mn}=\frac{1}{4}\Big[3F(\frac{m}{M},\frac{n}{N})-F(\frac{m+1}{M},\frac{n+1}{N})+ F(\frac{m+1}{M},\frac{n}{N})+F(\frac{m}{M},\frac{n+1}{N})\Big] \tag{20}$$

$$b_{mn}=\frac{M}{2}\Big[F(\frac{m+1}{M},\frac{n}{N})-F(\frac{m}{M},\frac{n}{N})+ F(\frac{m+1}{M},\frac{n+1}{N})-F(\frac{m}{M},\frac{n+1}{N})\Big] \tag{21}$$

$$c_{mn}=\frac{N}{2}\Big[F(\frac{m}{M},\frac{n+1}{N})-F(\frac{m}{M},\frac{n}{N})+ F(\frac{m+1}{M},\frac{n+1}{N})-F(\frac{m+1}{M},\frac{n}{N})\Big] \tag{22}$$

$$\alpha_{mn}=\frac{1}{4}\Big[3\gamma(\frac{m}{M},\frac{n}{N})-\gamma(\frac{m+1}{M},\frac{n+1}{N})+ \gamma(\frac{m+1}{M},\frac{n}{N})+\gamma(\frac{m}{M},\frac{n+1}{N})\Big] \tag{23}$$

$$\beta_{mn}=\frac{M}{2}\Big[\gamma(\frac{m+1}{M},\frac{n}{N})-\gamma(\frac{m}{M},\frac{n}{N})+ \gamma(\frac{m+1}{M},\frac{n+1}{N})-\gamma(\frac{m}{M},\frac{n+1}{N})\Big] \tag{24}$$

$$\xi_{mn}=\frac{N}{2}\Big[\gamma(\frac{m}{M},\frac{n+1}{N})-\gamma(\frac{m}{M},\frac{n}{N})+ \gamma(\frac{m+1}{M},\frac{n+1}{N})-\gamma(\frac{m+1}{M},\frac{n}{N})\Big] \tag{25}$$

The polynomial results of ΔE_{mn} pertinent to four cases are shown by Eqs.(26)-(29), where L_{t} means a number very close to zero.

Case 1: $|\mathrm{j}k_{\mathrm{w}}\beta_{mn}|>L_{\mathrm{t}}$ and $|\mathrm{j}k_{\mathrm{w}}\xi_{mn}|>L_{\mathrm{t}}$

$$\Delta E_{mn}=\mathrm{e}^{\mathrm{j}k_{\mathrm{w}}\alpha_{mn}}\Bigg\{a_{mn}\frac{\mathrm{e}^{\mathrm{j}k_{\mathrm{w}}\beta_{mn}/M}-1}{\mathrm{j}k_{\mathrm{w}}\beta_{mn}}\cdot\frac{\mathrm{e}^{\mathrm{j}k_{\mathrm{w}}\xi_{mn}/N}-1}{\mathrm{j}k_{\mathrm{w}}\xi_{mn}}+ b_{mn}\Bigg[\frac{\mathrm{e}^{\mathrm{j}k_{\mathrm{w}}\beta_{mn}/M}}{\mathrm{j}k_{\mathrm{w}}\beta_{mn}M}-\frac{\mathrm{e}^{\mathrm{j}k_{\mathrm{w}}\beta_{mn}/M}-1}{(\mathrm{j}k_{\mathrm{w}}\beta_{mn})^2}\Bigg]\frac{\mathrm{e}^{\mathrm{j}k_{\mathrm{w}}\xi_{mn}/N}-1}{\mathrm{j}k_{\mathrm{w}}\xi_{mn}}+ c_{mn}\frac{\mathrm{e}^{\mathrm{j}k_{\mathrm{w}}\beta_{mn}/M}-1}{\mathrm{j}k_{\mathrm{w}}\beta_{mn}}\Bigg[\frac{\mathrm{e}^{\mathrm{j}k_{\mathrm{w}}\xi_{mn}/N}}{\mathrm{j}k_{\mathrm{w}}\xi_{mn}N}-\frac{\mathrm{e}^{\mathrm{j}k_{\mathrm{w}}\xi_{mn}/N}-1}{(\mathrm{j}k_{\mathrm{w}}\xi_{mn})^2}\Bigg]\Bigg\} \tag{26}$$

Case 2: $|\mathrm{j}k_{\mathrm{w}}\beta_{mn}|<L_{\mathrm{t}}$ and $|\mathrm{j}k_{\mathrm{w}}\xi_{mn}|>L_{\mathrm{t}}$

$$\Delta E_{mn}=\sum_{p=0}^{\infty}\frac{(\mathrm{j}k_{\mathrm{w}}\beta_{mn})^p}{p!}\mathrm{e}^{\mathrm{j}k_{\mathrm{w}}\alpha_{mn}}\cdot \Bigg\{a_{mn}\frac{1}{(p+1)M^{p+1}}\cdot\frac{\mathrm{e}^{\mathrm{j}k_{\mathrm{w}}\xi_{mn}/N}-1}{\mathrm{j}k_{\mathrm{w}}\xi_{mn}}+$$

$$b_{mn}\frac{1}{(p+2)M^{p+2}}\cdot\frac{\mathrm{e}^{\mathrm{j}k_{\mathrm{w}}\xi_{mn}/N}-1}{\mathrm{j}k_{\mathrm{w}}\xi_{mn}}+ c_{mn}\frac{1}{(p+1)M^{p+1}}\left[\frac{\mathrm{e}^{\mathrm{j}k_{\mathrm{w}}\xi_{mn}/N}}{\mathrm{j}k_{\mathrm{w}}\xi_{mn}N}-\frac{\mathrm{e}^{\mathrm{j}k_{\mathrm{w}}\xi_{mn}/N}-1}{(\mathrm{j}k_{\mathrm{w}}\xi_{mn})^2}\right]\Bigg\} \quad (27)$$

Case 3: $|\mathrm{j}k_{\mathrm{w}}\beta_{mn}|<L_{\mathrm{t}}$ and $|\mathrm{j}k_{\mathrm{w}}\xi_{mn}|<L_{\mathrm{t}}$

$$\Delta E_{mn}=\sum_{p=0}^{\infty}\sum_{q=0}^{\infty}\frac{(\mathrm{j}k_{\mathrm{w}}\beta_{mn})^p}{p!}\cdot\frac{(\mathrm{j}k_{\mathrm{w}}\xi_{mn})^q}{q!}\mathrm{e}^{\mathrm{j}k_{\mathrm{w}}\alpha_{mn}}\cdot \left[a_{mn}\frac{1}{(q+1)N^{q+1}}\cdot\frac{1}{(p+1)M^{p+1}}+ b_{mn}\frac{1}{(q+1)N^{q+1}}\cdot\frac{1}{(p+2)M^{p+2}}+ c_{mn}\frac{1}{(q+2)N^{q+2}}\cdot\frac{1}{(p+1)M^{p+1}}\right] \quad (28)$$

Case 4: $|\mathrm{j}k_{\mathrm{w}}\beta_{mn}|>L_{\mathrm{t}}$ and $|\mathrm{j}k_{\mathrm{w}}\xi_{mn}|<L_{\mathrm{t}}$

$$\Delta E_{mn}=\sum_{p=0}^{\infty}\frac{(\mathrm{j}k_{\mathrm{w}}\xi_{mn})^p}{p!}\mathrm{e}^{\mathrm{j}k_{\mathrm{w}}\alpha_{mn}}\cdot \left\{a_{mn}\frac{1}{(p+1)N^{p+1}}\cdot\frac{\mathrm{e}^{\mathrm{j}k_{\mathrm{w}}\beta_{mn}/M}-1}{\mathrm{j}k_{\mathrm{w}}\beta_{mn}}+ b_{mn}\frac{1}{(p+1)N^{p+1}}\left[\frac{\mathrm{e}^{\mathrm{j}k_{\mathrm{w}}\beta_{mn}/M}}{\mathrm{j}k_{\mathrm{w}}\beta_{mn}M}-\frac{\mathrm{e}^{\mathrm{j}k_{\mathrm{w}}\beta_{mn}/M}-1}{(\mathrm{j}k_{\mathrm{w}}\beta_{mn})^2}\right]+ c_{mn}\frac{1}{(p+2)N^{p+2}}\cdot\frac{\mathrm{e}^{\mathrm{j}k_{\mathrm{w}}\beta_{mn}/M}-1}{\mathrm{j}k_{\mathrm{w}}\beta_{mn}}\right\} \quad (29)$$

In Eq.(26), as $|\mathrm{j}k_{\mathrm{w}}\beta_{mn}|=0$ and $|\mathrm{j}k_{\mathrm{w}}\xi_{mn}|=0$ are two singular points thus causing a problem of singularity in numerical calculation, the singular terms in Eq.(26) should be expanded in Taylor series to settle it. Similarly, the ΔE_{mn} from Eq.(27) to Eq.(29) for the other three cases are shown in a like series. In Refs.[10]-[11], the conditions $|\mathrm{j}k_{\mathrm{w}}\gamma_{mn}|<L_{\mathrm{t}}$ and $|\mathrm{j}k_{\mathrm{w}}\gamma_{mn}|>L_{\mathrm{t}}$ under which the above four cases are assigned seem to cut no ice with Taylor series expansion of the singular terms in Eq.(26), while the conditions $|\mathrm{j}k_{\mathrm{w}}\xi_{mn}|<L_{\mathrm{t}}$ and $|\mathrm{j}k_{\mathrm{w}}\xi_{mn}|>L_{\mathrm{t}}$ advanced in this article appear to be more reasonable.

A pre-partitioning process using the proposed polynomial representation of NURBS is needed in order to set up different parametric sub-domains $[m/M,\ (m+1)/M]\times[n/N,\ (n+1)/N]$, where the phase term $k_{\mathrm{w}}\gamma(u,v)$ can be expressed by a simple bivariate linear form. The computational accuracy of the modified Ludwig's algorithm for NURBS is determined by the selected values of M and N which can be determined by a phase term variation constraint. Practically, for a fixed value of u, the difference between $k_{\mathrm{w}}\gamma(m/M,\ n/N)$ and $k_{\mathrm{w}}\gamma(m/M,\ (n+1)/N)$ cannot exceed a threshold (for example, ±1 rad); and for a fixed value of v, the difference between $k_{\mathrm{w}}\gamma(m/M,\ n/N)$ and $k_{\mathrm{w}}\gamma((m+1)/M,\ n/N)$ cannot exceed the same threshold. The accuracy of the results of ΔE_{mn} is improved when the values of M and N increase.

4. Numerical Results

Numerical results of RCS for two different geometries are presented in the following part.

Fig.2 shows a circular flat plate with a radius of R = 1 m, centered at the origin of Cartesian coordinates. The backscattered RCS of the circular flat plate depends only on the aspect angle θ due to the circular symmetry, and the frequency of the incident field is 10 GHz. The results from the proposed approach are presented in Fig.3, where they are compared with those in Ref.[16] which used an analytical representation of the backscattered RCS of the circular flat plate.

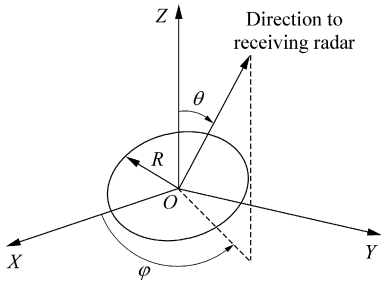

Fig.2 A circular flat plate.

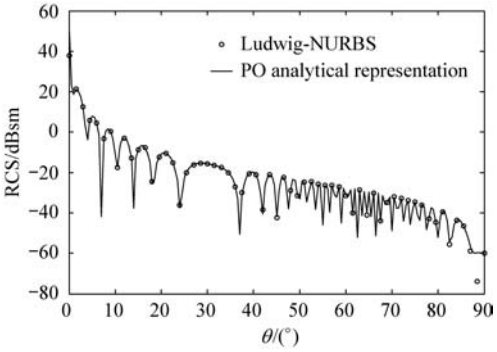

Fig.3 Monostatic RCS of a circular flat plate.

Fig.4 illustrates an ellipsoid centered at (0,0,0) m and defined by

$$x^2+\frac{y^2}{4}+\frac{z^2}{9}=1$$

The frequency of the incident wave is 10 GHz. The monostatic RCS in a cut with $\varphi=45°$ is computed (see Fig.5). The effectiveness of the proposed method is verified against the results obtained with the PO analytical representation of the ellipsoid backscattered RCS given by Ref.[16].

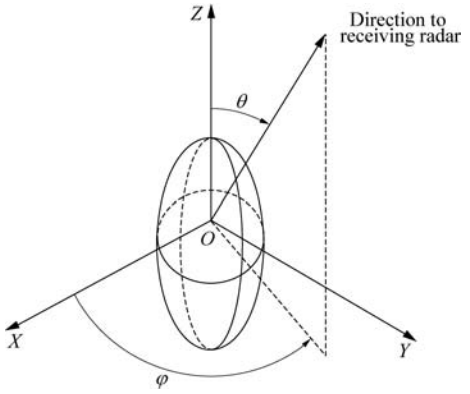

Fig.4 An ellipsoid.

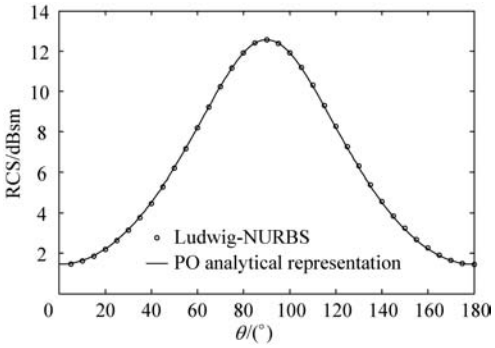

Fig.5 Monostatic RCS of an ellipsoid vs aspect angle θ ($\varphi = 45°$).

5. Conclusions

This article applies the physical optics method to the monostatic RCS calculation of electrically large conducting objects modeled by NURBS surfaces. A polynomial representation of B-spline basis functions is presented to make NURBS surfaces more suitable for numerical computation, and a modified Ludwig's algorithm is adopted to calculate the PO integrals over NURBS surfaces. This proposed method provides a useful tool for high-frequency RCS computation. In addition, the polynomial representation of B-spline basis functions can be used together with other quasi-analytical tools such as the stationary phase integration method for the NURBS-based PO integral evaluation.

References

[1] Perez J, Catedra M F. Application of physical optics to the RCS computation of bodies modeled with NURBS surfaces. IEEE Trans Antennas Propagat 1994; 42(10): 1404-1411.

[2] Perez J, Saiz J A, Conde O M, et al. Analysis of antennas on board arbitrary structures modeled by NURBS surfaces. IEEE Trans Antennas Propagat 1997; 45(6): 1045-1053.

[3] Wang N, Liang C H, Yuan H B. Calculation of pattern in UTD method based on NURBS modeling with the source on surface. Microwave and Optical Technology Letters 2007; 49(10): 2492-2498.

[4] Conde O M, Perez J, Catedra M F. Stationary phase method application for analysis of radiation of complex 3-D conducting structures. IEEE Trans Antennas Propagat 2001; 49(5): 724-731.

[5] Hu J L, Lin S M, Wang W B. Computation of PO integral on NURBS surface and its application to RCS calculation. Electronics Letters 1997; 33(3): 239-240.

[6] Roedder J M. CADDSCAT version 2.3: a high-frequency physical optics code modified for trimmed IGES B-spline surfaces. IEEE Antennas Propagat Magazine 1999; 41(3): 69-80.

[7] Tan Y. Computation of PO integral on parametric surfaces. International Journal of Infrared and Millimeter Waves 2001; 22(12): 1795-1804.

[8] Catedra M F, Delgado C, Luceri S, et al. Efficient procedure for computing fields created by current modes. Electronics Letters 2003; 39(10): 763-765.

[9] Delgado C, Gomez J M, Catedra M F. Analytical field calculation involving current modes and quadratic phase expressions. IEEE Trans Antennas Propagat 2007; 55(1): 233-240.

[10] Wang M, Chen M, Liang C H. Ludwig algorithm's improvement and its application on NURBS-PO method. IEEE International Symposium on Microwave, Antenna, Propagation and EMC Technologies for Wireless Communications (MAPE2005). 2005; 258-260.

[11] Wang M, Wang N, Liang C H. Problem of singularity in Ludwig's algorithm. Microwave and Optical Technology Letters 2007; 49(2): 400-403.

[12] Adana F S, Diego I G, Blanco O G, et al. Method based on physical optics for the computation of the radar cross section including diffraction and double effects of metallic and absorbing bodies modeled with parametric surfaces. IEEE Trans Antennas Propagat 2004; 52(12): 3295-3303.

[13] Catedra M F, Delgado C, Diego I G. New physical optics approach for an efficient treatment of multiple bounces in curved bodies defined by an impedance boundary condition. IEEE Trans Antennas Propagat 2008; 56(3): 728-736.

[14] Shi F Z. CAGD&NURBS. Beijing: Higher Education Press, 2001; 265-270. [in Chinese]

[15] Piegl L, Tiller W. The NURBS book. 2nd ed. New York: Springer-Verlag, 1997; 50-51, 128-129.

[16] Mahafza B R. Radar systems analysis and design using MATLAB. New York: Chapman & Hall, 2000; 85-89.

Biographies:

Fang Xiang Born in 1981, he is now a Ph.D. candidate in School of Electronics and Information Engineering, Beijing University of Aeronautics and Astronautics. His main research interests lie in computational electromagnetics and analysis of radar target characteristics.
E-mail: xiangfangit@ee.buaa.edu.cn

Su Donglin Born in 1960, she is now a professor and a supervisor of Ph.D. candidates in School of Electronics and Information Engineering, Beijing University of Aeronautics and Astronautics. Her main research interests include EMC/EMI problems, antenna and array design, and numerical methods of electromagnetics.
E-mail: sdl@buaa.edu.cn